

Electronic structure of Janus layers based on $\text{Ti}_{1-y}\text{Cr}_y(\text{Se}_{1-x}\text{S}_x)_2$

© D.V. Beliaev¹, Yu.E. Kovalenko¹, A.A. Titov¹, V.A. Golyashov^{2,3}, O.E. Tereshchenko^{2,3},
R.G. Chumakov⁴, A.N. Titov¹, T.V. Kuznetsova^{1,5}

¹ M.N. Mikheev Institute of Metal Physics, Ural Branch, Russian Academy of Sciences,
620137 Yekaterinburg, Russia

² Rzhanov Institute of Semiconductor Physics, Siberian Branch, Russian Academy of Sciences,
630090 Novosibirsk, Russia

³ Synchrotron Radiation Facility — Siberian Circular Photon Source „SKIF“ Boreskov Institute
of Catalysis of Siberian Branch of the Russian Academy of Sciences,
630559 Koltsovo, Russia

⁴ National Research Center „Kurchatov Institute“,
123182 Moscow, Russia

⁵ Ural Federal University after the first President of Russia B.N. Yeltsin,
620002 Yekaterinburg, Russia

E-mail: danil.belyaev08@gmail.com

Received April 19, 2024

Revised October 16, 2024

Accepted April 16, 2024

Single crystals $\text{Ti}_{0.9}\text{Cr}_{0.1}(\text{Se}_{0.8}\text{S}_{0.2})_2$ and $\text{Ti}_{0.85}\text{Cr}_{0.15}(\text{Se}_{0.8}\text{S}_{0.2})_2$ were synthesized for the first time by gas-transport reactions. The structural and phase purity of the obtained single crystals was investigated by X-ray powder diffraction. The chemical composition of the synthesized samples was determined by energy dispersive X-ray spectroscopy on a scanning electron microscope. The electronic structure was studied by ARPES method. With increasing Cr concentration, a decrease in conduction band filling and a decrease in hole mass is observed. The absence of dispersion-free band is also observed, which indicates the absence of metal intercalation into the interlayer space.

Keywords: janus structures, angle-resolved photoemission spectroscopy, transition metal dichalcogenides.

DOI: 10.61011/SC.2024.07.59541.6333H

1. Introduction

Transition metal dichalcogenides are layered materials with a general formula MX_2 ($M = \text{Ti}, \text{Zr}, \text{Mo}, \text{Hf}; X = \text{S}, \text{Se}, \text{Te}$). The atoms are bonded together by ion-covalent bond inside the layer and a Van der Waals bond is formed between the layers as quasi-2D structures, and explore various effects related to the samples dimensions. Transition metal dichalcogenides are featuring such unique properties as superconductivity [1,2], charge-density waves [1,3], topology [1,4], that allow using them in a wide range of applications such as in electronics [5], lithium batteries [6] and photodetectors [7]. One of the ways to modify the properties of these compounds is the intercalation of atoms or molecules into the interlayer space [8]. Another way to change the properties of dichalcogenides is substitution in the metal sub-lattice [9]. In paper [10] it was shown that in $\text{Ti}_{1-x}\text{Cr}_x\text{Se}_2$ compounds a stoichiometric metal evolves, mainly Ti, in the inter-layer space when substituting the four-valence titanium (Ti^{4+}) by a trivalent chromium (Cr^{3+}), which results in disruption of the quasi-2D structure. Therefore, in order to prevent self-intercalation and preserve the quasi-2D structure, additional electrons shall be introduced in the system. This will make it possible to completely replace titanium with chromium [11] without forming an excess transition metal between the layers.

Janus structures have attracted tremendous scientific interest recently due to the emergence of new unique properties that arise from the breaking of mirror symmetry due to different atoms on each side of their unit cell in such materials [12–14]. These compounds may be synthesized based on the transition metals dichalcogenides when substituting Se by S or visa versa, where $\text{S}-M-\text{Se}$ structure represents itself a Janus layer. In paper [15] for $\text{TiSe}_2-\text{TiS}_2$ system practically unlimited solubility of components was demonstrated. This is due to the similarity of their electronic and crystal structures. Both compounds have a trigonal lattice with a spatial group $P-3m1$ (№ 164), however, they have different parameters: $a_0 = 3.407 \text{ \AA}$ and $c_0 = 5.680 \text{ \AA}$ for TiS_2 ; $a_0 = 3.528 \text{ \AA}$ and $c_0 = 5.981 \text{ \AA}$ for TiSe_2 . These materials also have similar electronic structure: TiS_2 is a narrow-bandgap semiconductor with indirect band gap ($\sim 0.5 \text{ eV}$), where the apex of valence band is formed by p -orbital of the chalcogen atoms in Γ -point of Brillouin zone (BZ), and the bottom of conduction band was formed by $3d$ states of titanium in M-point of BZ; for TiSe_2 the apex of valence band and the bottom of the conduction band are formed in a similar way that for TiS_2 , while the gap value being no higher than 0.05 eV . In paper [16] it was shown that there are no features in the spectra of angle-resolved photoelectron spectroscopy (ARPES) in $\text{TiSe}_{2-x}\text{S}_x$ compounds when substituting up to $x = 0.34$, except for

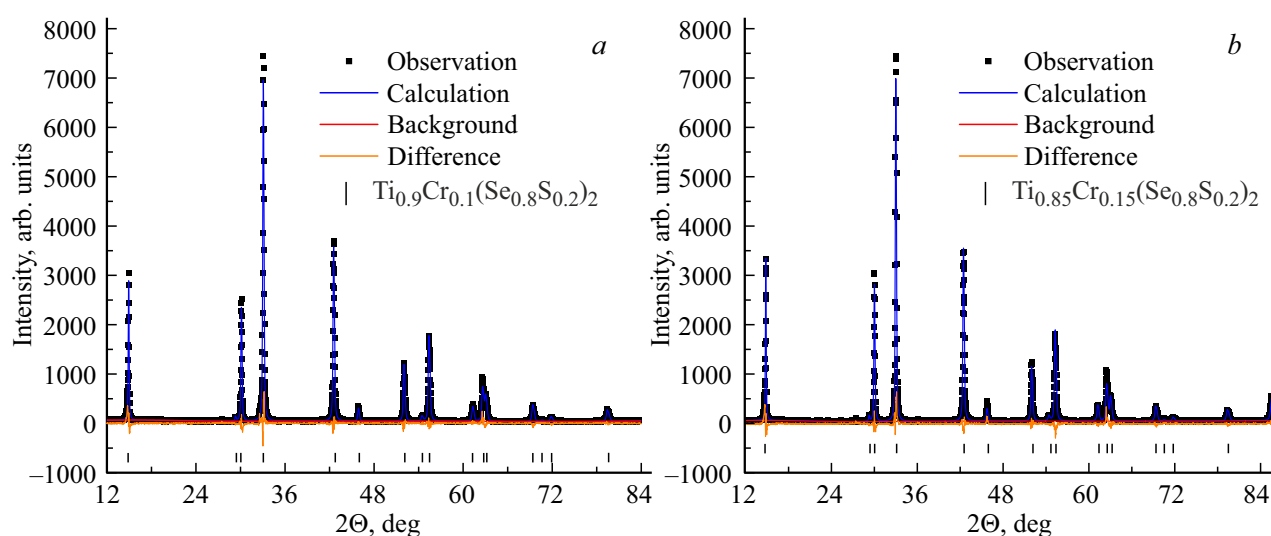


Figure 1. Full-profile analysis of powder X-ray diffraction for samples $\text{Ti}_{0.9}\text{Cr}_{0.1}(\text{Se}_{0.8}\text{S}_{0.2})_2$ (a) and $\text{Ti}_{0.85}\text{Cr}_{0.15}(\text{Se}_{0.8}\text{S}_{0.2})_2$ (b).

the gradual change of the band gap width between Γ –M direction of BZ. Later, in paper [17] when analyzing EMF dependence of electrochemical cell $\text{Li}/\text{Li}^+/\text{Ti}(\text{Se}_{1-x}\text{S}_x)_2/\text{Pt}$ the EMF of the cell was found to be reduced by 0.5 eV, both, in substitution of S by Se, and in substitution of Se by S at level of substitution $x = 0.2$. Since, in the studied compound there are no atoms of Li, variation of EMF is associated with Fermi energy growth in $\text{Ti}(\text{Se}_{1-x}\text{S}_x)_2$. The observed increase in Fermi energy may be manifested due to a donor nature of Janus structures because of Laplace pressure, since substitution of Se by S is isovalent, but due to different ionic radii there may occur lattice curvature. Hence, we may expect, that Janus structures in $\text{Ti}_{1-y}\text{Cr}_y(\text{Se}_{1-x}\text{S}_x)_2$ compounds will allow substituting Ti by Cr without additional intercalation of metal into the inter-layer space. Yet, it remains unclear how many donor electrons are generated due to the formation of Janus layers.

In the study $\text{Ti}_{1-y}\text{Cr}_y(\text{Se}_{1-x}\text{S}_x)_2$ single-crystals were synthesized for the first time by gas transport reactions from the prepared polycrystalline charge. The structural and phase purity of polycrystals was studied by X-ray powder diffraction (XPD). Chemical composition of single-crystals was studied using the energy-dispersive X-ray analysis (EDX). Electronic structure of single-crystals was studied using angle-resolved photoelectron spectroscopy (ARPES).

2. Materials and research techniques

Polycrystalline samples $\text{Ti}_{0.85}\text{Cr}_{0.15}(\text{Se}_{0.8}\text{S}_{0.2})_2$ and $\text{Ti}_{0.9}\text{Cr}_{0.1}(\text{Se}_{0.8}\text{S}_{0.2})_2$ were synthesized from highly pure elements (3N) weighed according to stoichiometric ratio. Polycrystalline charge was synthesized in quartz vacuum ampoules (10^{-5} Torr) at 900°C for 5 days. The resulting compounds were then mechanically ground in a mortar and pressed to improve contact. The resulting compressed

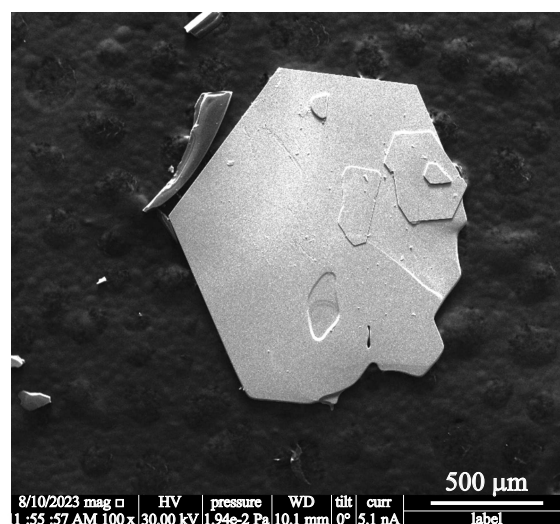


Figure 2. SEM-image of single-crystal $\text{Ti}_{0.85}\text{Cr}_{0.15}(\text{Se}_{0.8}\text{S}_{0.2})_2$.

samples were annealed in vacuumed ampoules for 5 days at a temperature of 750°C . Single-crystal samples were grown from polycrystalline charge by gas transport reactions with Se as a carrier. Chemical composition of single-crystals was determined by EDX method using a scanning electron microscope Quanta 200 at the Shared Research Facility of IMP UB RAS. The structure and phase purity of synthesized single-crystals were studied by XPD method using XRD 7000 Maxima diffractometer, $\text{CuK}\alpha = 1.5418 \text{ \AA}$ ($\Delta x < 5\%$). ARPES-measurements were made along Γ –M direction of Brillouin zone at a temperature of 80 K and pressure below 10^{-10} mbar using photoelectron spectroscopy system SPECS Proven-X ARPES fitted with helium UV gas-discharge source UVS-300 ($h\nu = 21.22 \text{ eV}$) and hemispherical analyzer

of electrons energy ASTRAIOS 190, in ISP SB RAS. The samples were cleaved in the ultrahigh vacuum ($< 10^{-10}$ mbar) at room temperature. Low-energy electron diffraction (LEED) was used to characterize the long-range crystal order, as well as to determine the directions of high symmetry on the surface of the samples after cleavage.

3. Results and discussion

Powder X-ray diffraction and full-profile analysis for $\text{Ti}_{0.85}\text{Cr}_{0.15}(\text{Se}_{0.8}\text{S}_{0.2})_2$ and $\text{Ti}_{0.9}\text{Cr}_{0.1}(\text{Se}_{0.8}\text{S}_{0.2})_2$ compounds are shown in Figure 1. Based on the results of a full-profile analysis, the single-phase nature of the synthesized systems was determined. Spatial group of $P-3m1$ (№ 164) compounds, parameters of unit cell for $\text{Ti}_{0.85}\text{Cr}_{0.15}(\text{Se}_{0.8}\text{S}_{0.2})_2$ are $a = 3.513 \text{ \AA}$, $c = 5.930 \text{ \AA}$, $V = 63.399 \text{ \AA}^3$, for $\text{Ti}_{0.9}\text{Cr}_{0.1}(\text{Se}_{0.8}\text{S}_{0.2})_2$ are $a = 3.513 \text{ \AA}$, $c = 5.941 \text{ \AA}$, $V = 63.515 \text{ \AA}^3$. The level of self-intercalation upon results of a full-profile analysis doesn't exceed 4.5%.

Figure 2 illustrates an appearance of a typical single-crystal grown during synthesis. From EDX-analysis it was found the studied single-crystals have minor deviations from stoichiometry $\text{Ti}_{0.87}\text{Cr}_{0.13}(\text{Se}_{0.77}\text{S}_{0.23})_{1.87}$ instead of $\text{Ti}_{0.85}\text{Cr}_{0.15}(\text{Se}_{0.8}\text{S}_{0.2})_2$ and $\text{Ti}_{0.91}\text{Cr}_{0.09}(\text{Se}_{0.78}\text{S}_{0.22})_{1.85}$ instead of $\text{Ti}_{0.9}\text{Cr}_{0.1}(\text{Se}_{0.8}\text{S}_{0.2})_2$.

Figure 3 shows the ARPES data for single-crystals $\text{Ti}_{0.85}\text{Cr}_{0.15}(\text{Se}_{0.8}\text{S}_{0.2})_2$ and $\text{Ti}_{0.9}\text{Cr}_{0.1}(\text{Se}_{0.8}\text{S}_{0.2})_2$ in Γ -M direction of BZ. A dispersion dependence is observed, which is an evidence of the crystalline quasi-2D structure of samples and the absence of self-intercalation. The indirect band gap of $\sim 0.08 \text{ eV}$ is also observed. Additionally, a displaced area in the valence band in Γ -point of BZ is observed. This displaced area may be attributed to the formation of Cr-containing Janus structures.

The observed stoichiometry deviations may be caused by the error of method used to determine the chemical composition of a sample or by the presence of intercalated metal in the inter-layer space, since the ratio of Ti to Cr, similar to the ratio of Se to S, is close to the required value, however, $Me : Ch = 1 : 2$ ratio is not preserved (here, Me is deemed as a joint content of Cr and Ti atoms, and Ch — joint content of Se and S atoms). In our case, the first option is most likely, since the XPD results show that self-intercalation into the interlayer space does not exceed 4.5% and there are no dispersion-free zones peculiar to the intercalated atoms in the ARPES spectra. According to the analysis of ARPES spectra, there is a decline in the intensity of the signal from the bottom of the conduction band with higher chromium content in the samples, which is associated with the substitution of Ti by Cr in the metal sub-lattice, and there is also a decrease in the effective mass of holes as the chromium concentration rises, i.e. $m_{\text{holes-Cr0.15}} < m_{\text{holes-Cr0.1}}$, since zone dispersion for a sample containing $\text{Cr}_{0.1}$, is higher compared to a sample containing $\text{Cr}_{0.15}$.

4. Conclusion

The single-crystals $\text{Ti}_{0.85}\text{Cr}_{0.15}(\text{Se}_{0.8}\text{S}_{0.2})_2$ and $\text{Ti}_{0.9}\text{Cr}_{0.1}(\text{Se}_{0.8}\text{S}_{0.2})_2$ were synthesized for the first time by method of gas transport reactions. Based on the results of a full-profile analysis, the single-phase nature of the samples is shown and the parameters of the unit cell are determined. The chemical composition of the synthesized single crystals was determined using EDX analysis. The deviation from the stoichiometric ratio is due to the error of the method. According to ARPES data, the absence of a dispersion-free zone has been established, which indicates the absence of metal intercalation into the interlayer space. The presence of the indirect band gap $\sim 0.08 \text{ eV}$ was

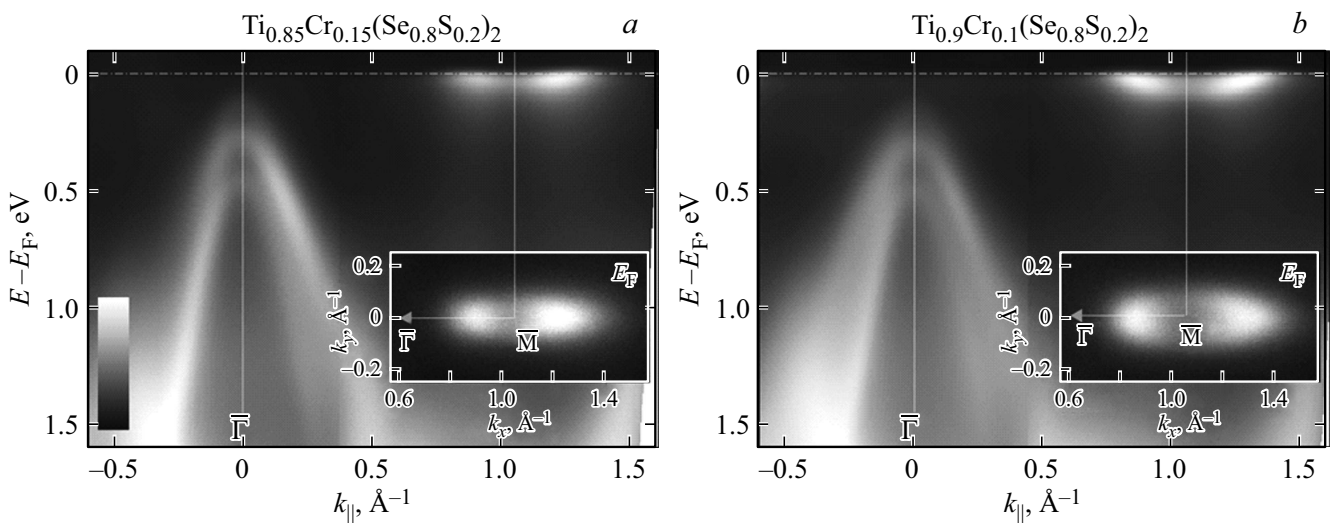


Figure 3. ARPES spectra for surface of single-crystals $\text{Ti}_{0.85}\text{Cr}_{0.15}(\text{Se}_{0.8}\text{S}_{0.2})_2$ (a) and $\text{Ti}_{0.9}\text{Cr}_{0.1}(\text{Se}_{0.8}\text{S}_{0.2})_2$ (b), measured in $\text{M}-\Gamma-\text{M}$ direction at $T = 80 \text{ K}$, $h\nu = 21.22 \text{ eV}$. The inserts show the corresponding maps of the Fermi surface near M-point.

demonstrated. Additionally, a displaced area is observed that may be associated with the formation of Cr-containing Janus structures. A decrease in the signal intensity at the bottom of the conduction band was revealed with an increase in the chromium concentration in the sample, which is associated with the substitution of Ti atoms by Cr atoms in the metal sub-lattice, and a decrease in the mass of holes as the concentration of chromium atoms goes up.

Funding

The study has been funded by a grant of the Russian Science Foundation No. 23-72-00067. Authors (SRF „SKIF“ V.A. Golyashov and O.E. Tereschenko) express their thanks to RF Ministry of Science and Higher Education for the financial support within the state assignment of SRF „SKIF“ Institute of Catalysis SB RAS.

Conflict of interest

The authors declare that they have no conflict of interest.

References

- [1] S. Manzeli, D. Ovchinnikov, D. Pasquier, O.V. Yazyev, A. Kis. *Nature Rev. Mater.*, **2**, 1 (2017).
- [2] W. Shi, J. Ye, Y. Zhang, R. Suzuki, M. Yoshida, J. Miyazaki, N. Inoue, Y. Saito, Y. Iwasa. *Sci. Rep.*, **5**, 12534 (2015).
- [3] P. Chen, Y.-H. Chan, X.-Y. Fang, Y. Zhang, M.Y. Chou, S.-K. Mo, Z. Hussain, A.-V. Fedorov, T.-C. Chiang. *Nature Commun.*, **6**, 8943 (2015).
- [4] M.K. Hooda, C.S. Yadav, D. Samal. *J. Phys.: Condens. Matter*, **33**, 103001 (2020).
- [5] J. Yu, C.-H. Lee, D. Bouilly, M. Han, P. Kim, M.L. Steigerwald, X. Roy, C. Nuckolls. *Nano Lett.*, **16**, 3385 (2016).
- [6] S. Fan, X. Zou, H. Du, L. Gan, C. Xu, W. Lv, Y.-B. He, Q.-H. Yang, F. Kang, J. Li. *J. Phys. Chem. C*, **121**, 13599 (2017).
- [7] K. Zhang, X. Fang, Y. Wang, Y. Wan, Q. Song, W. Zhai, Y. Li†, G. Ran, Y. Ye, L. Dai. *ACS Appl. Mater. Interfaces*, **9**, 5392 (2017).
- [8] N. Sirica, S.-K. Mo, F. Bondino, I. Pis, S. Nappini, P. Vilmercati, J. Yi, Z. Gai, P.C. Snijders, P.K. Das, I. Vobornik, N. Ghimire, M.R. Koehler, L. Li, D. Sapkota, D.S. Parker, D.G. Mandrus, N. Mannella. *Phys. Rev. B*, **94**, 075141 (2016).
- [9] A.S. Shkvarin, Y.M. Yarmoshenko, A.I. Merentsov, E.G. Shkvarina, A.F. Gubkin, I. Piš, S. Nappini, F. Bondino, I.A. Bobrikov, A.N. Titov. *Inorg. Chem.*, **59**, 8543 (2020)
- [10] A.N. Titov, A.I. Merentsov, V.N. Neverov. *Phys. Solid State*, **48**, 1472 (2006).
- [11] J.M. Tarascon, F.J. DiSalvo, M. Eibschutz, D.W. Murphy, J.V. Waszczak. *Phys. Rev. B*, **28**, 6397 (1983).
- [12] A. Kandemir, H. Sahin. *Phys. Rev. B*, **97**, 155410 (2018).
- [13] J. Zhang, S. Jia, I. Kholmanov, L. Dong, D. Er, W. Chen, H. Guo, Z. Jin, V.B. Shenoy, L. Shi, J. Lou. *ACS Nano*, **11**, 8192 (2017).
- [14] D.B. Trivedi, G. Turgut, Y. Qin, M.Y. Sayyad, D. Hajra, M. Howell, L. Liu, S. Yang, N.H. Patoary, H. Li, M.M. Petric, M. Meyer, M. Kremser, M. Barbone, G. Soavi, A.V. Stier, K. Müller, S. Yang, I.S. Esqueda, H. Zhuang, J.J. Finley, S. Tongay. *Adv. Mater.*, **32**, 2006320 (2020).
- [15] R. Nitsche. *Fortschr. Miner.*, **44**, 231 (1967).
- [16] M.-L. Mottas, T. Jaouen, B. Hildebrand, M. Rumo, F. Vanini, E. Razzoli, E. Giannini, C. Barreteau, D.R. Bowler, C. Monney, H. Beck, P. Aebi. *Phys. Rev. B*, **99**, 155103 (2019).
- [17] A.N. Titov, A.S. Shkvarin, A.I. Merentsov, O.V. Bushkova, E.A. Suslov, A.A. Titov, J. Avila, M.C. Asensio, N.V. Kazantseva, M.S. Postnikov. *Chem. Mater.*, **33**, 8915 (2021).

Translated by T.Zorina